TOWARDS BEAM-DYNAMICS SIMULATIONS INCLUDING MORE REALISTIC FIELD DESCRIPTIONS FOR THE HESR

J. Hetzel*[1], U. Bechstedt, J. Böker, A. Lehrach[1,2], B. Lorentz, R. Tölle
Institute for Nuclear Physics 4 (IKP-4), Forschungszentrum Jülich, Germany
[1]also at Physics Institute III B, RWTH Aachen University, Germany
[2]also at JARA-FAME (Forces and Matter Experiments), Jülich Aachen Research Alliance, Germany

Abstract

The High Energy Storage Ring (HESR) is part of the upcoming Facility for Antiproton and Ion Research (FAIR) in Darmstadt (Germany). The HESR is designed for antiprotons with a momentum range from 1.5 GeV/c to 15 GeV/c, but will as well be suitable to provide heavy ion beams with a momentum range from approximately 0.6 GeV/c to 5.8 GeV/c. To guarantee smooth operation it is crucial to verify and improve the design with beam-dynamics simulations. Particularly the dynamic aperture is calculated as a measure of quality.
Complementary to previous beam dynamics calculations based on frequency map analysis [1], the dynamic aperture is calculated using a variant of the Lyapunov exponent. The first bending and focusing magnets have been delivered and the magnetic fields measured recently. So the assumed values of the the multipole imperfections used so far in the machine model are now replaced by values based on field measurements.

INTRODUCTION

Subject of this paper is the estimation of the short term dynamic aperture for the HESR [2]. All calculations are based on the so-called injection lattice for antiprotons. Here the kinetic energy of the antiprotons at injection is 3 GeV, the transition energy of the lattice is set to $\gamma_{tr} = 6.2$. The calculations are based on tracking studies performed with the PTC module of MAD-X [3].
Objective of the current studies is a tune scan for this setting to identify areas of large dynamic aperture, i.e. minimal influences of non-linearities. The main sources for these non-linearities, besides the sextupole fields for chromaticity correction, are the harmonic imperfections of the bending dipoles and the quadrupoles. Both types of magnets are in the series production state. Thus measurements of the harmonic content of the elements as quality assurance, as well as basis for the tracking studies are performed.

MEASUREMENT OF THE HARMONIC CONTENT

Immediately after production of each of the in total 84 normal conducting quadrupoles a measurement of the harmonic content is performed by the manufacturer. This is done by the use of a rotating coil. The used layout is a radial coil with analogue bucking of the main field component. The analysis of the measured data is performed following [4], including rotational and feed down correction to correct for misalignments. The measurements result in a description of the transverse field of the quadrupole integrated along the longitudinal axis of the element:

$$B_y + iB_x = \sum_{n=1}^{\infty} (\mathcal{B}_n + i\mathcal{A}_n) \left(\frac{x + iy}{r_0} \right)^{n-1} . \qquad (1)$$

Here $\mathcal{B}_n$ and $\mathcal{A}_n$ are the so-called multipole coefficients at reference radius r_0. Usually they are normalized to the main field component $\mathcal{B}_N$. In case of a quadrupole this results in

$$b_n + ia_n = \frac{\mathcal{B}_n + i\mathcal{A}_n}{\mathcal{B}_2} \cdot 10^4. \qquad (2)$$

The measured harmonic content averaged over the 33 elements that are measured up to now is shown in Fig. 1. Based on the measured values as well as the measured standard deviation from element to element a random set of multipole components is generated for each of the 84 quadrupoles in the HESR lattice. This set is used later on to describe the element imperfection in the tracking studies. The measured values are not used directly for two reasons: First of all up to now not all elements are produced not to mention measured,

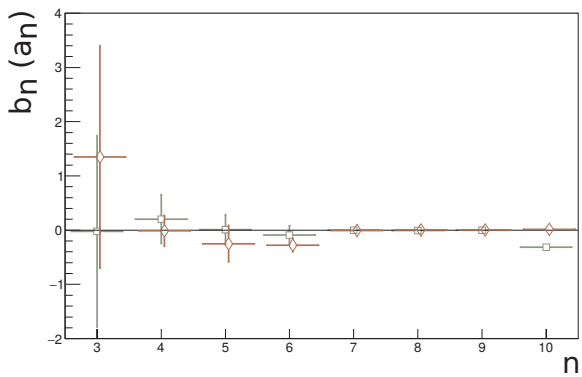

Figure 1: The harmonic content of the quadrupole. The error bars indicate the statistic fluctuations between the different elements. The upright multipole components b_n are labelled with a square marker and the skew multipole components a_n are labelled with a diamond marker. To separate the markers of the normal and skew multipoles the skew multipoles are slightly shifted to the right. The reference radius is $r_0 = 33$ mm.

* j.hetzel@fz-juelich.de

ISBN 978-3-95450-147-2

second the statistically distributed harmonic coefficients tend to change if the element is dissassembled and reassembled e.g. to insert the beam tube. The set of the randomized multipoles can be variied by choosing a different random seed.

The bending magnets (in total there will be 44 normal conducting sector dipoles) cannot be measured by the use of rotating coils as the elements are bent. Instead it is planned to use a Hall device that moves through the magnet. This device measures the tangential as well as the azimuthal components of the field on the surface of a bent cylinder. The bending radius corresponds to the curvature of the magnet. Again a description in multipole components as in Eq. (1) is desired. This can be achieved by a Fourier transformation of the measured values.

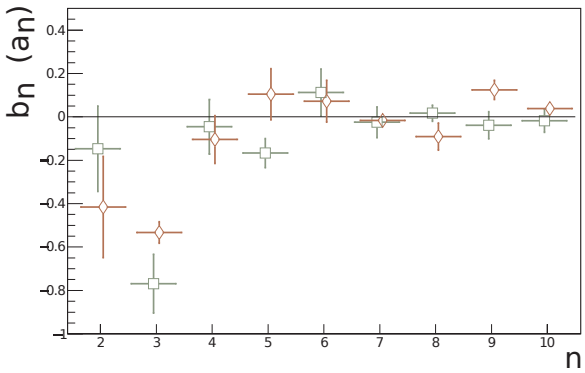

Figure 2: The harmonic content of the bending dipoles as used in the beam dynamics simulations. The values are based on preliminary proof of concept measurements as described in [5]. The upright multipole components b_n are labelled with a square marker and the skew multipole components a_n are labelled with a diamond marker. To separate skew and normal markers all skew markers are slightly shifted to the right. The error bars represent the repeatability of the measurement. The reference radius is $r_0 = 30\,\mathrm{mm}$.

As the device is still under development, the basis for the multipole components of the dipoles in the beam dynamics simulation is the proof of concept measurement with a single Hall probe that is described in [5]. The result of this measurement is shown in Fig. 2. For the simulation the multipoles are again randomized according to the measured values.

TRACKING

Starting from the linear lattice without disturbances by the multipole errors, a tune scan is performed. For a tune range $Q_x, Qy \in [7.57, 7.76]$ a geometric acceptance of $A_x, A_y > 15\,\mathrm{mm\,mrad}$ can be achieved without completely altering the linear lattice. The resulting acceptances are given in Fig. 3. In this range the dynamic aperture is estimated by tracking including the multipole errors. As the area is rather large only a short term tracking with 1000 turns per initial point

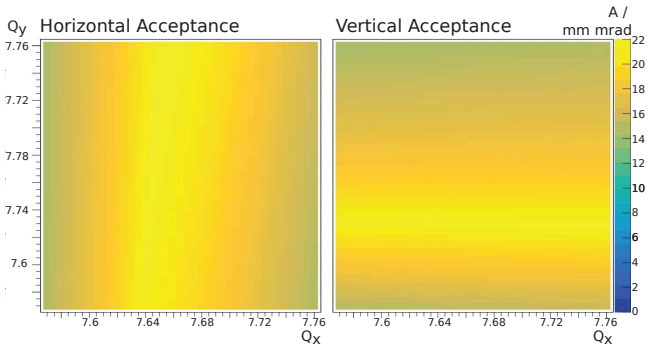

Figure 3: The geometric acceptance as defined by the linear lattice of the HESR. On the left the horizontal acceptance versus the tune is given in greyscale (colour on-line). On the right the same plot for the vertical acceptance is given.

in phase space is performed. The settings of the tracking environment are summarised in Table 1.

Table 1: Tracking Settings

Setting	Value
Tracking Environment	PTC module of MAD-X
Description of Elements	Matrix-Kick-Matrix
Slices per Element	8
Included Multipoles	$n \leq 10$
Hamiltonian	approximated
Number of Tracked Turns	1000

Lyapunov Indicator

As an estimate for the dynamic aperture a modified version of the Lyapunov indicator λ as introduced in [6] is used:

$$\lambda(n) := \frac{\bar{d}_{n/2,n} - \bar{d}_{0,n/2}}{\bar{d}_{n/4,3n/4}}. \tag{3}$$

Here n denotes the number of tracked turns and $\bar{d}_{i,j}$ is the average distance of two initially close-by particles within turns i and j.

As a conservative estimate for the dynamic aperture the tracked motion is considered as chaotic if $\lambda(n)$ exceeds 1 during the tracking. Hereby the first 100 turns are neglected to suppress transient effects. So the motion is considered to be stable if

$$\lambda(n) \leq 1,\ \forall n \in (100, 1000]. \tag{4}$$

For each point in tune space an initial point in phase space with

$$\vec{z}_i = \begin{pmatrix} x_i \\ p_{x,i} \\ y_i \\ p_{y,i} \end{pmatrix} = 0.01 \cdot \begin{pmatrix} a_x \cdot \sqrt{A_x/\gamma_x(s=0)} \\ 0\,\mathrm{mrad} \\ a_y \cdot \sqrt{A_y/\gamma_y(s=0)} \\ 0\,\mathrm{mrad} \end{pmatrix} \tag{5}$$

is set. Initially the coefficients a_x and a_y are set to 1; $s = 0$ refers to the longitudinal starting point of the tracking. If

ISBN 978-3-95450-147-2

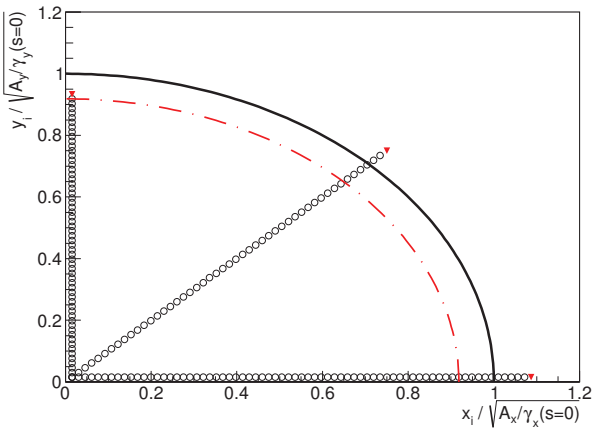

Figure 4: Example of initial points in space. The balls denote initial points where Eq. (4) was not violated, whereas the triangles denote the onset of chaotic motion. The bold line is the geometric acceptance limit scaled to the longitudinal starting point of the tracking. The resulting dynamic aperture estimate is given as dashed line.

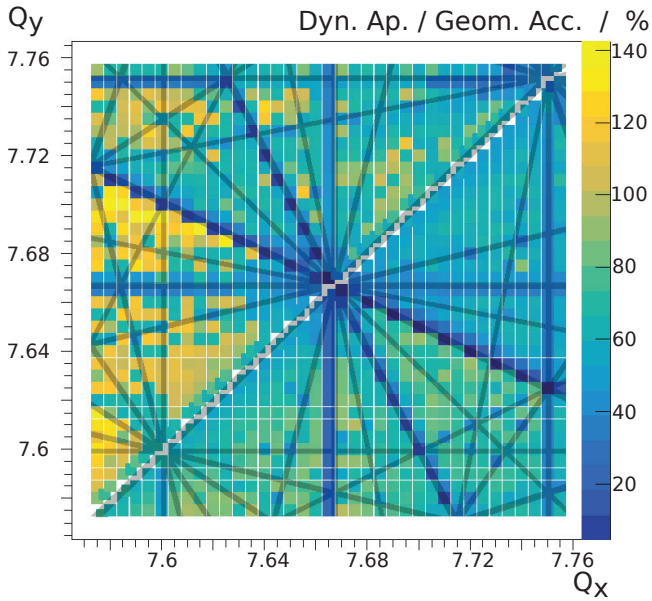

Figure 5: Resulting dynamic aperture from tune scan. The dynamic aperture is plotted in greyscale (colour on-line).

the stability criterion Eq. (4) is not violated, a_x or a_y are increased by approximately 1.5. As sketched in Fig. 4 in total three series of tracking are performed: One where just a_x is increased, one where a_x and a_y are increased simultaneously and one where just a_y is increased. As the tracking serves just as a conservative estimate, the minimal radius $r = \sqrt{x_i^2 + y_i^2}$ at which the motion, according to Eq. (4), changes from stable to chaotic defines the dynamic aperture.

Results

The results of the tune scan are shown in Fig. 5. There, for each pair of horizontal and vertical tunes the dynamic aperture is estimated. The results are also compared to the tune resonances up to multipole order $n = 6$. As expected, the tunes with low dynamic aperture coincide with these resonances. Additionally, it can be seen that the tunes near the coupling resonance $Q_x = Q_y$ can not be reached during tracking. This is due to the non-vanishing skew quadrupole component of the bending magnets. In previous studies for the HESR, such as [1], this was not seen, as skew multipole components of the bending magnets were not considered. Tune combinations with large dynamic aperture identified in Fig. 5 serve as initial points for future investigations, such as long term tracking.

CONCLUSION

The model of the HESR could be extended to include realistic field descriptions based on measurements. Short term tracking and application of the Lyapunov criterion, Eq. (4), are appropriate to identify restrictions to the acceptance limit caused by non-linearities.

REFERENCES

[1] D.M. Welsch, A. Lehrach, B. Lorentz, R. Maier, D. Prasuhn and R. Tölle, "Investigation and Optimization of Transverse Non-Linear Beam Dynamics in the High-Energy Storage Ring HESR", in *Proc. 1st Int. Particle Accelerator Conf. (IPAC'10)*, Kyoto, Japan, May 2010, paper THPE063, pp. 4659–4661.

[2] R. Maier for the HESR Consortium, "The High-Energy Storage Ring (HESR)", in *Proc. of 2011 Particle Accelerator Conf. (PAC'11)*, New York, USA, March 2011, paper THOCN2, pp. 2104–2106.

[3] H. Grote, F. Schmidt, L. Deniau, G. Roy, "The MAD-X Program (Methodical Accelerator Design) - User's Reference Manual", *Version 5.02.09, preliminary draft*, CERN, Geneva, Switzerland, April 2016.

[4] L. Bottura, et al., "Standard Analysis Procedures for Field Quality Measurement of the LHC Magnets - Part I: Harmonics", *LHC Project Document No. LHC-M-ES-0007 rev 1.0*, CERN, Geneva, Switzerland, November 2001.

[5] J. Hetzel, "Measurement of the Harmonic Content of the HESR Dipoles with a Single 3D Hall Probe", in *Annual Report 2015 of IKP, Forschungszentrum Jülich*, Jülich, Germany, 2016, chapter K - Further contributions, p. 87.

[6] T. L. Rijoff, F. Zimmermann, "Simulating the Wire Compensation of LHC Long-Range Beam-Beam Effects", in *Proc. 11th International Computational Accelerator Physics Conf. (ICAP 2012)*, Rostock-Warnemünde, Germany, August 2012, paper WESA I3, pp. 135–137.

ISBN 978-3-95450-147-2